



# General Cluster Sorption Isotherm

Christoph Buttersack

*Institute for Non-Classical Chemistry at Leipzig University, Permoserstr. 15, 04318, Leipzig, Germany*

## ARTICLE INFO

### Keywords:

Modeling  
Adsorption isotherm  
Argon  
Nitrogen  
Capillary condensation  
Ordered mesoporous silica  
MCM-41  
Nonporous silica  
NLDFT  
QSDFT

## ABSTRACT

Adsorption isotherms are an essential tool in chemical physics of surfaces. However, several approaches based on a different theoretical basis exist and for some isotherms existing approaches can fail. Here, the sorbate-sorbate interaction is not limited to an orientation vertical to the adsorbent surface. Instead, a formal orientation-independent clustering, also comprising the possibility of multilayers as a special case, is underlain. The flexible clusters are described by classical thermodynamics including a free energy relationship depending on the cluster size. In this paper a rigorous unified treatment of the adsorbate-adsorbate-adsorbent interaction is shown to result in a general isotherm equation which is applied to literature data both concerning type IV isotherms of argon and nitrogen in ordered mesoporous silica, and type II isotherms of disordered macroporous silica. The new isotherm covers the full range of partial pressure ( $10^{-6}$  - 0.7). The determination of surface areas is not possible by this isotherm because the cross-sectional area of a cluster is unknown. Based on the full description of type IV isotherms, most known isotherms including BET are accessible by respective simplifications. The presented model is an extension of the classical derivation of the  $\zeta$ -isotherm which was shown to describe type IV isotherms restricted to adsorbates with very strong tendency of clustering such as water on hydrophobic surface (Phys. Chem. Chem. Phys. 21 (2019) 5614).

## 1. Introduction

A sorption isotherm is the result of molecular interaction between individual molecules with a surface and with these adsorbed molecules among each other. Traditionally, sorbate-sorbate interactions are described by lateral forces or multilayer formation [1]. More general and elegant is the concept of 3-dimensional clusters which can merge and form a surface attached liquid film or fill the confined space of mesopores [2,3]. The resulting isotherm of mesopore-filling has a sigmoidal shape and is known as type IV in the IUPAC classification [4]. It can be regarded as the most complex isotherm comprising all known other isotherms as respective simplifications. That complexity is only outreached by the existence of several distinct adsorption sites. In that heterogeneous case the adsorption has to be treated as an additive superposition of homogeneous patches [5]. Science in that direction culminates in the proposal of “universal isotherms” to be fitted to sorption on any porous body, but they are limited to local Langmuir type adsorption [6]. The curve fitting results then in a characteristic energy distribution of the adsorbent [7]. Instead, the focus of the present article is the basic nature of sorbate-sorbate interaction on homogeneous surface (patches).

Here we concentrate on subsequent processes starting with the

adsorption of low concentrated and isolated molecules on an ideal plane surface via clustering to capillary condensation. These isotherms are of special interest for the determination of pore size distributions by sorption of argon or nitrogen at their boiling temperature. Modern methods rely on the classical density functional theory (DFT) being a part of statistical mechanics [8]. The adsorbate molecules are simplified as hard spheres in front of the rigid adsorbent surface. Liquid-solid interaction is modeled by two parameters of a Lennard-Jones (LJ) potential resulting from fitting to non-porous surfaces while the LJ potential of the liquid-liquid interaction is usually determined to reproduce the equation of state of the bulk fluid [8]. Recent DFT versions are extended by an excess hard sphere attractive term. The non-local density functional theory (NLDFT) consists of an additional “smooth density approximation” [9], while the quenched solid density functional theory (QSDFT) formally treats the solid surface as a mixture of a solid and a fluid leading to a characteristic solid density profile [10]. These methods do not only allow the determination of pore sizes: modeling of adsorption isotherm is accomplished, too. However, NLDFT isotherms do only roughly follow the experimental basis; they are characterized by artificial steps [8]. QSDFT isotherms reproduce the experiment much better [11–13] but a significant deviation can occur in the very low pressure region [10].

E-mail address: [christoph.buttersack@uni-leipzig.de](mailto:christoph.buttersack@uni-leipzig.de).

<https://doi.org/10.1016/j.micromeso.2021.110909>

Received 13 December 2020; Received in revised form 4 January 2021; Accepted 12 January 2021

Available online 7 February 2021

1387-1811/© 2021 Elsevier Inc. All rights reserved.

Beside this sophisticated modeling simpler versions exist for sigmoidal isotherms. Semi-empirical approaches are reviewed [3,14] and extended by a new contribution [15]. A recently proposed cluster formation model [3] stems from biochemistry. It is based on the thermodynamic equilibrium of multiple ligand-receptor complexes introduced by Klotz [16,17] and lastly has its root in the Langmuir-analog Michaelis-Menten [18,19] concept. It was assumed in the cluster formation model [3] that the primary sorption step, necessary for the final clustering, can be described by only one parameter.

Based on this successive thermodynamical equilibrium a  $\beta$ -fold clustering with the primary sorption constant  $K_1$  and the cluster formation constant  $K$  is established, and the degree of coverage  $\theta$  as a function of the partial pressure  $x$  is derived [3] to be

$$\theta(x) = \frac{K_1 x + 2 K_1 K_2 x^2 + 3 K_1 K_2 K_3 x^3 + \dots + n (K_1 K_2 K_3 \dots K_n) x^n}{1 + K_1 x + K_1 K_2 x^2 + K_1 K_2 K_3 x^3 + \dots + (K_1 K_2 K_3 \dots K_n) x^n} \quad (4)$$

$$\theta_\beta = \frac{C_1 (Kx) \{ 1 - (1 + \beta) (Kx)^\beta + \beta (Kx)^{\beta+1} \}}{(1 - (Kx)) \{ 1 + (C_1 - 1) (Kx) - C_1 (Kx)^{\beta+1} \}} \quad (1)$$

where  $C_1$  is given by

$$C_1 = K_1/K \quad (2)$$

That equation is identical with the  $\zeta$ -isotherm of Ward et al. [20] derived by statistical thermodynamics.

Equation (1) was found to describe numerous type IV and V experimental isotherms [3]. However, its validity is restricted to a special case of type IV adsorption where the interaction with the pore walls is extremely weak or restricted to few defect regions whereas the adsorbate self-interaction is high. A prominent example is the adsorption of water in hydrophobic microporous carbon [2]. However, the application of equation (1) fails drastically for a lot of type IV isotherms, especially in case of the very important adsorption on ordered mesoporous materials. An example is shown in the Supplementary Information (SI) in Figure S2. To solve that problem, a more general version of equation (1) with more degree of freedom is presented hereinafter.

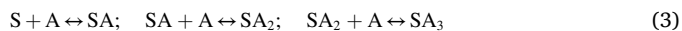
## 2. Methods

All experimental data stem from the literature. Nonlinear regressions, using the Levenberg-Marquardt algorithm [21], were performed by a program written in R [22] with the implemented package of minpack.lm [23]. Since the variation of the fit parameter  $\alpha$  is limited to natural numbers, its optimization could not be subsumed to the Levenberg-Marquardt method but had to be realized by an extra subroutine. All nonlinear regressions were performed with reciprocal weight of the processed adsorption values. Depending on the experimental data the numbers of the power functions, occurring during intermediate states of the regression program, can exceed the common limits of  $10^{-300}$  and  $10^{+300}$ . This had to be considered during programming by multiplying the numbers with appropriate factors. In some cases ( $N_2$  sorption on MCM-41) a commercial nonlinear regression program (Sigmaplot) was utilized in addition, since it allows a somewhat higher span of numbers compared to the minpack.lm package of R. Sigmaplot, however, does not support the incorporation of loops in its programming tools.

## 3. Results and discussion

### 3.1. General isotherm

The following derivation starts with the isotherm of Klotz [16,17] originally developed for the evaluation of interactions between proteins and inorganic or small organic molecules in liquid water. When S is a primary binding site (protein) and A the molecule to be adsorbed, the multi-site binding is described by



and so on. The respective equilibrium constants  $K_1, K_2, K_3$  are given by the concentration of S, A,  $SA_1, SA_2, SA_3$  etc. so that the number of ligands bound per protein is derived to be

where  $x$  is the concentration of A. Although that concept has been originally applied to strongly bound complexes, mostly by coulombic interactions, it can be extended to (weak) physical adsorption, too. A prominent example is the derivation of the BET isotherm of Brunauer, Emmett, and Teller [24]. Another example is the analogous description of solvation in liquids [25]. Hereinafter,  $\theta$  is therefore regarded as the adsorbed amount per formal monolayer ranging from 0 to  $\beta$ . To emphasize the limitation of  $\beta$  to finite values, the corresponding  $\theta$  is indexed as  $\theta_\beta$ , in contrast to  $\theta$  which includes the limit  $\beta \rightarrow \infty$ .

To reduce the number of symbols in the following equations and to be in line with the notation used in a previous publication [3], the final cluster formation constant  $K$  (already presented in eqn. (1) of the introduction and discussed later on) is introduced, and  $x$  is replaced by

$$q = Kx \quad (5)$$

Furthermore the products  $K_1 K_2, K_1 K_2 K_3$  etc. are replaced by

$$C_n = \frac{1}{K^n} \prod_{i=1}^n K_i \quad (6)$$

The notation of  $C$  is applied to highlight its linkage to the  $C$ -value traditionally used in the BET equation [24] (see section 3.6. later on). Using these definitions eqn. (4) can be written as

$$\theta_\beta(q) = \frac{\sum_{n=1}^{\beta} n C_n q^n}{1 + \sum_{n=1}^{\beta} C_n q^n} \quad (7)$$

Mathematically this equation is defined for natural but not infinite numbers of  $n$  and  $\beta$ , for real numbers of  $C_n$ , and  $0 \leq q < \infty$ .

Within a thermodynamic treatment, not only the degree of coverage but also the surface tension characterizes the sorption equilibrium. The surface tension  $\pi$  is given by Gibbs' equation [1].

$$\pi = RT \int_0^x \frac{\theta}{x} dx \quad (8)$$

which can also be written as

$$\pi = RT \int_0^q \frac{\theta}{q} dq \quad (9)$$

After inserting  $\theta$  from eqn. (7) into eqn. (9) the following integral is obtained

$$\pi_\beta = RT \int_0^1 \frac{\sum_{n=1}^{\beta} n C_n q^{n-1}}{1 + \sum_{n=1}^{\beta} C_n q^n} dq \quad (10)$$

Since the numerator is the exact first derivative of the denominator, the integral can be easily solved:

$$\pi_\beta = \ln \left( 1 + \sum_{n=1}^{\beta} C_n q^n \right) \quad (11)$$

The denominator of equation (7) can therefore be read as a separate thermodynamic measure. The surface tension increases with the cluster size  $n$ .

This description of a general multiple equilibrium is now transferred to a capillary condensation process. In the foregoing publication [3] the adsorption on the primary sites was assumed to be defined only by  $K_1$ ,

$$\theta_\beta(q) = \frac{(1-q)^2 \sum_{n=1}^{\alpha} n C_n q^n + q C_\alpha ((\alpha+1) q^\alpha - (\beta+1) q^\beta + \beta q^{\beta+1} - \alpha q^{\alpha+1})}{(1-q)^2 \left( 1 + \sum_{n=1}^{\alpha} C_n q^n \right) + (1-q) C_\alpha (q^{\alpha+1} - q^{\beta+1})} \quad (18)$$

and all other constants from  $K_2$  to  $K_\beta$  were responsible for the clustering within the capillary condensation. In that case all values of  $K_n$  beside  $K_1$  are equal and given by the final cluster formation constant  $K$ . In contrast, it is assumed here that the primary sorption is defined not only by  $K_1$  but by  $K$ -values ranging from  $K_1, K_2, K_3, \dots$  to  $K_\alpha$ . When  $K_\alpha$  is reached, the capillary condensation proceeds with  $K$ , so that

$$K = K_\alpha \quad (12)$$

while  $K$  is constant during the further increase of cluster size  $n$ . In case of a type IV isotherm, the sequence of  $K_n$  should monotonously decrease because the first element of the cluster is adsorbed strongest and the following elements more and more loose so long until the constant  $K$  is reached. An analogous behavior results for  $C_n$ . According to eqn. (6) these values build a monotonously increasing sequence ranging from  $C_1$  to  $C_\alpha$  which is then the maximal value at all.

The following transformations aim at the separation of the geometric sums in one with different  $C$  values ranging from  $C_1$  to  $C_\alpha$ , and another with  $C_n = C_\alpha$  for  $\alpha+1 \leq n \leq \beta$ . At first the numerator of eqn. (7) is considered and split into

$$\sum_{n=1}^{\beta} n C_n q^n = \sum_{n=1}^{\alpha} n C_n q^n + C_\alpha \sum_{n=\alpha+1}^{\beta} n q^n \quad (13)$$

For  $q \neq 1$  the last term can be transformed to [26]

$$\begin{aligned} \sum_{n=\alpha+1}^{\beta} n q^n &= \sum_{n=1}^{\beta} n q^n - \sum_{n=1}^{\alpha} n q^n = \\ &= \frac{q(1 - (\beta+1)q^\beta + \beta q^{\beta+1})}{(1-q)^2} \\ &\quad - \frac{q(1 - (\alpha+1)q^\alpha + \alpha q^{\alpha+1})}{(1-q)^2} \\ &= \frac{q((\alpha+1)q^\alpha - (\beta+1)q^\beta + \beta q^{\beta+1} - \alpha q^{\alpha+1})}{(1-q)^2} \end{aligned} \quad (14)$$

The denominator of eqn. (7) is split into

$$1 + \sum_{n=1}^{\beta} C_n q^n = 1 + \sum_{n=1}^{\alpha} C_n q^n + C_\alpha \sum_{n=\alpha+1}^{\beta} q^n \quad (15)$$

The last term can be transformed to [27].

$$\begin{aligned} \sum_{n=\alpha+1}^{\beta} q^n &= \sum_{n=1}^{\beta} q^n - \sum_{n=1}^{\alpha} q^n = \frac{q - q^{\beta+1}}{1-q} - \frac{q - q^{\alpha+1}}{1-q} \\ &= \frac{q^{\alpha+1} - q^{\beta+1}}{1-q} \end{aligned} \quad (16)$$

Based on the foregoing equations the full hybrid isotherm is

$$\theta_\beta(q) = \frac{\sum_{n=1}^{\alpha} n C_n q^n + \frac{q C_\alpha ((\alpha+1) q^\alpha - (\beta+1) q^\beta + \beta q^{\beta+1} - \alpha q^{\alpha+1})}{(1-q)^2}}{1 + \sum_{n=1}^{\alpha} C_n q^n + \frac{C_\alpha (q^{\alpha+1} - q^{\beta+1})}{1-q}} \quad (17)$$

or

Mathematically, this function is defined for  $\beta$  being natural numbers below infinite, for the natural numbers  $\alpha \leq \beta$ , and  $0 \leq q < \infty$  but  $q \neq 1$ . The value  $\theta_\beta(1)$  is obtained by the analog procedure starting from eqn. (7) (cf. SI)

$$\theta_\beta(1) = \frac{2 \sum_{n=1}^{\alpha} n C_n + C_\alpha \{ \beta(\beta+1) - \alpha(\alpha+1) \}}{2 \left\{ 1 + \sum_{n=1}^{\alpha} C_n + C_\alpha(\beta - \alpha) \right\}} \quad (19)$$

Eqns. (18) and (19) represent the general isotherm for  $\beta \neq \infty$ . A physically important property is that its slope is greater than zero at infinite small pressures  $x$ . As mathematically derived in the supporting information, Henry's condition

$$\lim_{q \rightarrow 0} \frac{d\theta_\beta}{dq}(q) = C_1 \quad \text{or} \quad \lim_{x \rightarrow 0} \frac{d\theta_\beta}{dx}(x) = K_1 \quad (20)$$

resp. is fulfilled. Significant is the behavior of  $\theta$  for  $q$  approximating infinite. As outlined in the SI for finite values of  $\beta$ , the following limits as  $q$  tends to infinity hold:

$$\lim_{q \rightarrow \infty} \theta_\beta(q) = \beta \quad (21)$$

$$\lim_{q \rightarrow \infty} \frac{d\theta_\beta}{dq}(q) = 0 \quad (22)$$

Further numerical analysis (cf. SI) reveals that the function bears a point of inflection typically ranging between  $0.980 < q < 0.999$  for  $\beta < \infty$  and monotonously increasing values of  $C_n(n)$ .

However, the isotherm equations (18) and (19) contain values of  $C_n$  which are not yet defined by any physical-chemical theory. A further general function for calculating  $C_n$  as a function of  $n$  is therefore required. Since  $C_n$  is defined through the product given in eqn. (6) via  $K_n$ , the problem would be solved by the knowledge of the principle course of the underlying energy distribution relative to the state at capillary condensation

with the Boltzmann constant  $k_B$ . It is the energy of the adsorption of clusters on a homogeneous surface.

### 3.2. Energy distribution

The energy should depend on the position of the clusters in front of the adsorbent surface and their size  $n$ . The state-of-the-art, however, is based on equations for surface and intermolecular potentials each of them based on power laws of inter-particle or particle-surface distances. For example, the exponent is 1 for coulombic, 3 for dipole-dipole and 6 for dispersive forces. Repulsion forces are taken into account by a term with the exponent 12 [28]. Thus, in statistical mechanics based methods of NLDFT and QSDFT a hard sphere approximation by the LJ potential

$$\varepsilon(r) = \varepsilon_{ff} \left\{ \left( \frac{\sigma_{ff}}{r} \right)^{12} - \left( \frac{\sigma_{ff}}{r} \right)^6 \right\} \quad (24)$$

is used for the intermolecular fluid-fluid interactions (ff) and analogously for the solid-fluid potential, too [8].

However, to solve the present question, the energy as a function of solely the molecules number  $n$  inside a cluster is required. In principle, that energy is accessible by a stepwise calculation of molecular interactions up to the cluster size  $n$ . Such an approach would require the solution of a non-additive many-body cluster expansion [29].

Here, however, the problem of the many-body expansion is skipped and an alternative concept is presented: The cluster itself is conceived as a flexible sphere having a virtual mass center and an effective radius  $r_c$  which again is defined by the molecular distance  $r_m$  and a shape factor  $\phi$ .

We assume the cluster is built by  $n$  molecules placed in a cubic lattice where their distance is  $2r_m$ . The volume of the cluster is then

$$v_c = n r_m^3 \quad (25)$$

It is further supposed that the basic cubes are arranged in a manner forming a sphere or more general an ellipsoid of revolution which has the volume

$$v_c = \frac{4\pi}{3} \phi^2 r_c^3 \quad (26)$$

with  $\phi$  being the ratio of lateral spacing parallel to the surface compared with  $r_c$  perpendicular to the surface. From the last two equations follows:

$$r_c = \left( \frac{3}{4\pi} \right)^{1/3} \frac{n^{1/3}}{\phi^{2/3}} r_m \quad (27)$$

This (asymmetric) cluster is thought to be an entity like a molecule. It is treated to have a virtual mass center and a distance  $r_c$  towards the adsorbent surface. The corresponding attraction energy  $\varepsilon_{sf}$  of the cluster or fluid (f) towards the surface (s) is now assumed to be proportional to the power law of  $r_c$  with the exponent  $3a$ .

$$\varepsilon_{sf} = \varepsilon_{sfo} \left( \frac{\sigma}{r_c} \right)^{3a} \quad (28)$$

Here  $\sigma$  is a scaling factor meaning that the potential is  $\varepsilon_{sfo}$  when  $\sigma$  is equal to  $r_c$ . Combining eqn. (27) and (28) results in

$$\varepsilon_{sf} = \varepsilon_{sfo} \left( \frac{4\pi}{3} \frac{\phi^2 \sigma^3}{r_m^3} \right)^a \left( \frac{1}{n} \right)^a \quad (29)$$

With the definition of

$$\sigma = \left( \frac{3}{4\pi} \frac{r_m^3}{\phi^2} \right)^{1/3} \quad (30)$$

and the assumption that the geometry factor  $\phi$  is independent on  $n$ , one obtains

$$\varepsilon_{sf} = \varepsilon_{sfo} \left( \frac{1}{n} \right)^a \quad (31)$$

meaning that  $\varepsilon_{sf}$  is equal to  $\varepsilon_{sfo}$  when the cluster size is unity. So far towards the energy of surface attraction.

Another energy term  $\varepsilon_{ff}$  is related to the energy of a molecule inside a cluster (liquid-like) compared to the isolated state (gas). The energy of any molecule inside the cluster is thought to be determined by its average distance towards the cluster mass center. At given geometry that value is proportional to  $r_c$  and we can analogously write

$$\varepsilon_{ff}(n) = \varepsilon_{ffo} \left( \frac{1}{n} \right)^b \quad (32)$$

This is the energy contribution of the cluster to only one molecule. For a multi-body system, where less than  $n$ -fold interactions are neglected, all these energies have to be multiplied [30]. Applying that rule also to the combination with the surface interaction (eqn. (31)) we obtain:

$$\varepsilon(n) = \varepsilon_{sfo} (\varepsilon_{ffo})^n \left( \frac{1}{n} \right)^a \left( \frac{1}{n} \right)^{b \cdot n} \quad (33)$$

$$\varepsilon(n) = \varepsilon_o \left( \frac{1}{n} \right)^{a+bn} \quad (34)$$

where  $\varepsilon_o$  is the energy at the beginning of the isotherm ( $q = 0$ ,  $n = 1$ ).

By combining equations (23) and (34) one obtains the energy relationship:

$$k_B T \ln \frac{K_n}{K} = \varepsilon_o \left( \frac{1}{n} \right)^{a+bn} \quad (35)$$

Remarkable is the inherent quite unusual power function  $n^n$ . The equivalent treatment of a single molecule and a cluster of these molecules is the core hypothesis of the concept used here. That analogy is manifest when describing the surface attraction of a cluster as interaction of the solid surface with the mass center of that cluster. Furthermore, it is important to note that eqn. (34) does not contain a term for repulsion potential because the cluster is thought to be a "soft sphere" which can completely evade these forces by changing its geometry [31]. When  $\phi = 1$ , the cluster is spherical, in case of  $\phi = 0$  it is completely flat.  $\phi$  comprises the possibility of transition states between the cluster and the layer concept. When the cluster is changed to a continuous phase it may be conceived to be delocalized. The essential definition of a cluster is the number of adsorbed molecules per primarily (with  $K_1$ ) adsorbed molecule. No further conditions are involved.

The derivation above shall provide an idea to understand the final  $\varepsilon(n)$  energy relationship (35). It needs to be compared with established theories or simulated, for example by quantum mechanics DFT [32] or classical statistical mechanics based Grand Canonical Monte Carlo [32].

### 3.3. Compatibility with conventional imaginations

The present concept for understanding sorption isotherms is a formal multi-equilibrium; but nevertheless it must be transferable to common imaginations of adsorption. The initial step is an attachment of a molecule at the adsorbent surface with the equilibrium constant  $K_1$  followed by further attachment on that molecule with  $K_2$ . A third reacts with these two, and so forth until  $K_n$ . Thus the clusters are built. During the initial phase of adsorption the clusters should be attached as separated islands while increasing coverage must result in cluster merging which may also be conceived as multilayer formation. The emergence of a continuous phase brings to the question of cluster geometry. One may assume that the isolated clusters will form a sphere. Will that sphere roll along the ideal plane of a homogeneous surface? Will that cluster deform, perhaps by migration of the first attachment point in analogy to a Grotthuss mechanism? When the attachment of the cluster is thought to be provided by only one cluster molecule, the covered fraction of surface is  $\theta_s = \theta/n$ , when the attachment points are conceived to be

completely delocalized, the covered surface is  $\theta_s = \theta$ , in reality it is in between:

$$\theta / n < \theta_s < \theta \quad (36)$$

This surface covering  $\theta_s$  has to be a function of  $\theta$ . But such a function cannot be deduced from the experimental isotherm. Further experimental information, especially the local surface tension, is missing. Only a special assumption allows the deduction of the covered surface from  $\theta$  alone: When one molecule is attached to the surface with  $K_1$  and the following ( $K_2, K_3 \dots K_n$ ) are positioned vertical to the surface, the value of  $\theta_s = \theta = 1$  would enable the calculation of the surface area based on a constant area required by one molecule. That imagination, being the basis of the BET multilayer concept [24], does not contradict to cluster formation. However, the full experimental pressure range is only very seldom described by this established model that separates surface interaction and layer formation by only one parameter. According to the literature, the BET method comprises an unsure molecular projection area [33], is shown to generally overestimate the surface area [34], and is at last a topic of further improvement [35]. Therefore, the BET surface area is rather defined by the application of a sound scientific standard than by measuring a physical entity [36].

Obviously, the influence of cluster geometry on the cluster projection area corresponds to the macroscopically observed wetting. The occurrence of droplets or spherical caps is therefore expected and found in Monte-Carlo simulations [37] depending on the strength of the first interaction and the cluster size. At last, the role of local surface tension and the theory of disjoining pressure [38,39] will help to understand cluster geometry and their merging into a continuous phase. The multilayer concept is preferred by imagination and suggests itself historically, but clustering may come to similar final imaginations. The superior of the more general cluster model is based on experimental results which are presented hereinafter.

### 3.4. Application to experimental type IV isotherms

In principle, the isotherm eqn. (18) alone can be used to fit

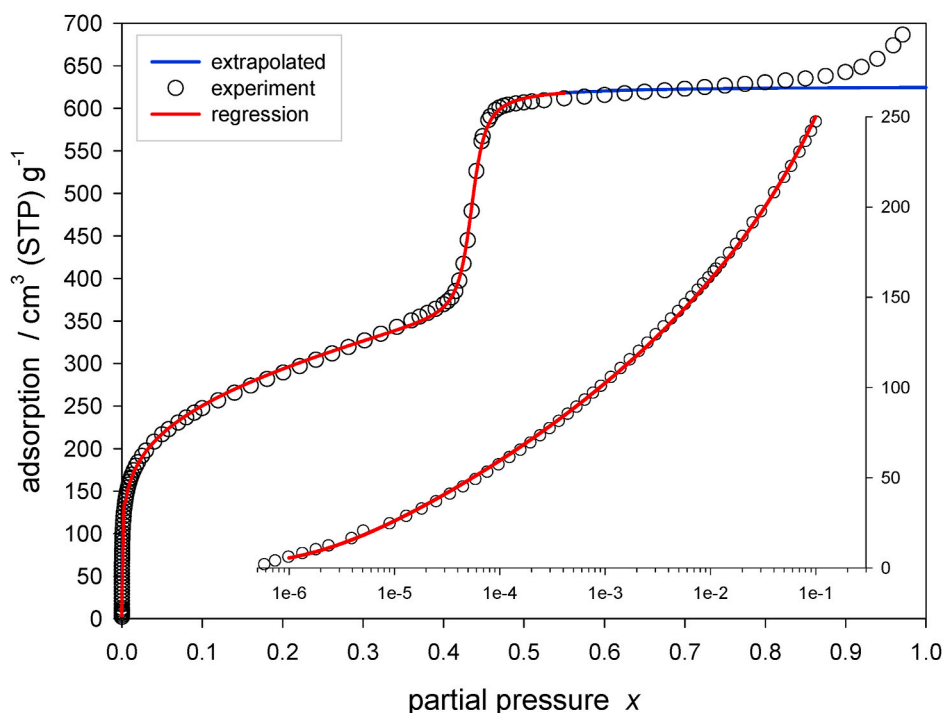


**Fig. 1.** Application of the General Cluster Sorption Isotherm (eqns. ((5), (18), (35) and (38))) to the adsorption of nitrogen (77 K) on siliceous MCM-41 (pore diameter 4.5 nm). Regression from  $x = 10^{-6}$  up to 0.6, extrapolated to  $x = 1$ . Data taken from supporting information of Kruk et al. [40].

experimental results. In that case the values of  $C_n$  or  $K_n$  resp. are free fit parameters so that fitting is difficult and fails when the cluster size  $n$  is greater than about 5. An example is presented in the SI (Figure S3). The resulting values of  $K_n$  were found to decrease with increasing  $n$ .

Stable nonlinear regressions were found when both the general isotherm (18) and the energy relationship (35) were used together. Based on these 2 equations a program for nonlinear regression has been written. The tested experimental data concerns the adsorption isotherm of nitrogen in ordered mesoporous silica of the type MCM-41 [40]. That type of material consists of cylindrical pores with a narrow pore size distribution [40]. Furthermore, the material has been calcined at 550 °C where isolated and geminal silanol groups should completely condense to cyclic trisiloxane [41]. The underlying samples should therefore be regarded as homogeneous, a condition which is very important for the validation of the theoretical background of the isotherm. Fig. 1 shows the good fit beginning at relative pressures of  $10^{-6}$  up to 0.7 including the steep increase at the relative pressure of 0.35 caused by capillary condensation. The positive deviation at higher pressure is due an additional secondary mesopore system which cannot be avoided by the synthesis conditions and is discussed in the publication of Kruk et al. [40] where the experimental data are taken from. The observed fit of the theoretical isotherm is much better than that attainable by NLDFT [8]. It can be compared with the accuracy of QSDFT isotherms [11–13].

Fig. 2 shows the course of the cluster size  $n$ . Starting at  $K_1$  the decrease is very strong and ends with  $K = K_{\alpha}$ . Note the logarithmic scale for  $K$  indicating that it is a measure of the free energy contribution of the step from  $n - 1$  to  $n$ . The course of  $\log C_n$  defined in equation (6), which is nothing else than the cumulated relative free energy up to  $n$ , is shown in Fig. 3. It is a hyperbolic function.

While the MCM-41 discussed above has 4.5 nm wide pores [40], another MCM with only 2.0 nm was investigated for nitrogen adsorption, too [42]. The excellent fit between theory and experiment is shown in the SI (Figure S4). Here the expected sharp increase caused by capillary condensation is nearly invisible. But the application of the new isotherm can resolve its existence.

The nitrogen isotherms were recorded at its boiling point at 77 K.



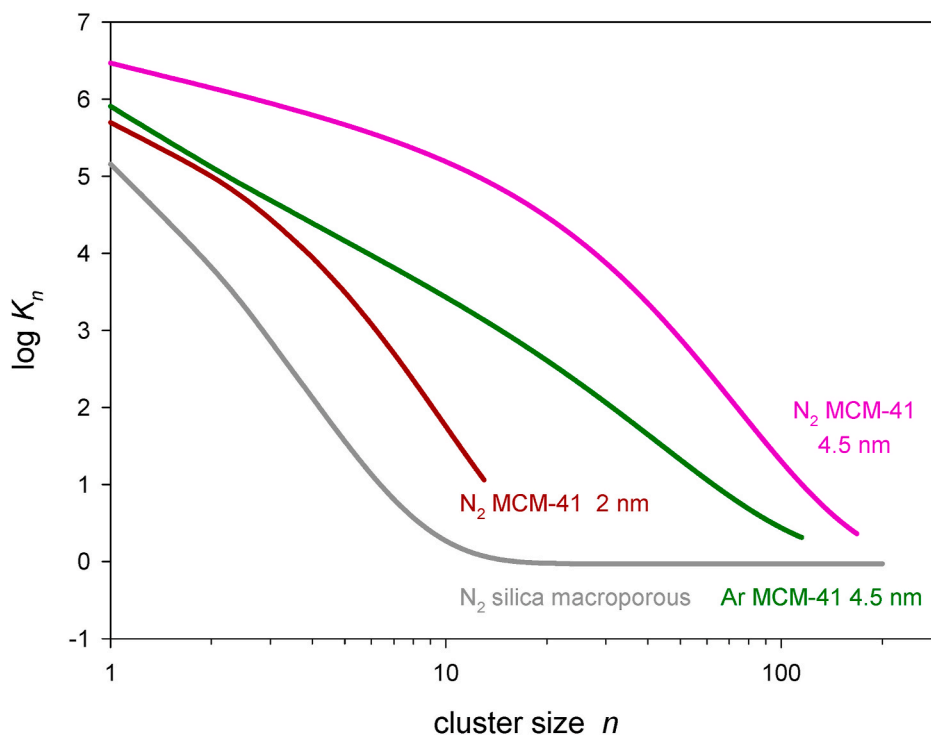


Fig. 2. Relative incremental free energy  $\log K_n$  as a function of the cluster size  $n$ .

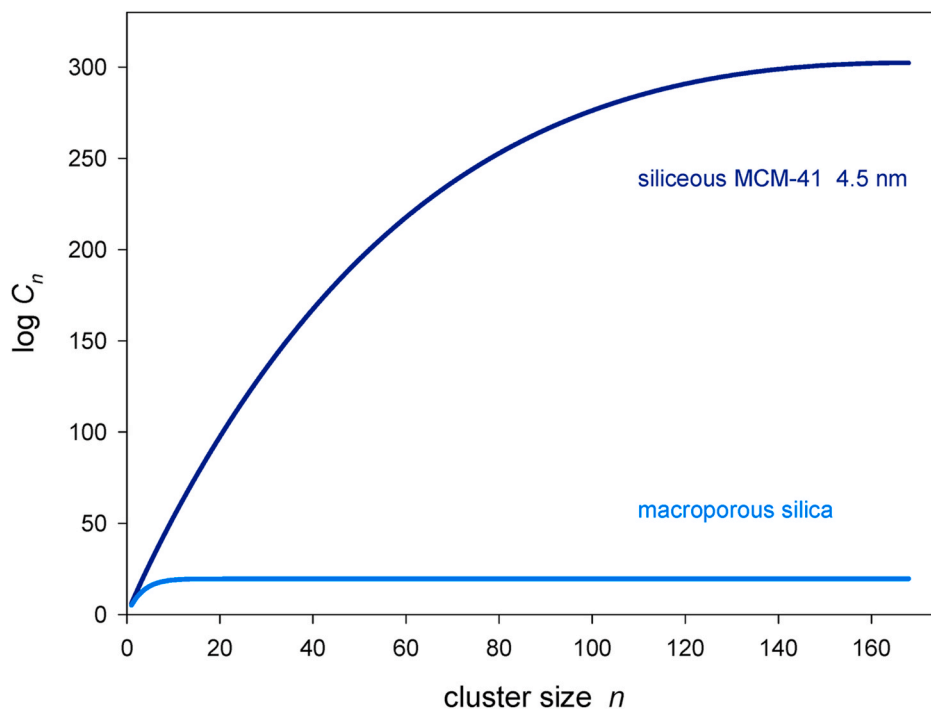


Fig. 3. Relative integral free energy  $\log C_n$  as a function of the cluster size  $n$ .

Another example shown in the SI (Figure S5) concerns the adsorption of argon at 77 K [43] which is a liquid in inside the 4.5 nm wide pore [44] at this temperature although its bulk phase melting point is 84 K. The calculated parameters are listed in Table 1. Beside the actual 6 model parameters  $K_1$ ,  $K$ ,  $\alpha$ ,  $\beta$ ,  $a$ , and  $b$ , the table also contains the absolute adsorption at the saturation stage  $Q_\infty$  as additional parameter, by which the adsorption in  $\text{cm}^3$  per g adsorbent  $Q$  is adjusted to the degree of coverage  $\theta_\beta$  with

$$Q = Q_\infty \theta_\beta / \beta \quad (37)$$

Another value corresponding to  $Q_\infty$  is the absolute adsorption  $Q_1$  where the degree of coverage is unity.

$$Q = Q_1 \theta_\beta \quad (38)$$

The values are  $Q_1 = 2.2 \text{ cm}^3 \text{ g}^{-1}$  for  $\text{N}_2$  and  $3.5 \text{ cm}^3 \text{ g}^{-1}$  for argon. At

**Table 1**

Parameters of the General Cluster Sorption Isotherm for type IV isotherms (eqns. (5), (18), (35) and (38)) and type II isotherms (eqns. (5), (35), (38) and (40)) as a result of its application to experimental isotherms from the literature [40,57,68].  $N$  is the number of experimental points used for regression and  $R$  the coefficient of determination.

adsorbent		$K_1$	$K$	$a$	$b$	$\alpha$	$\beta$	$Q_1/\text{cm}^3 \text{ (STP) g}^{-1}$	$N$	$R$
MCM-41, 4.5 nm	$\text{N}_2$ 77K	2.94E+06	$2.298 \pm 0.002$	$6.73\text{E-}02 \pm 2.8\text{E-}03$	$2.70\text{E-}03 \pm 5.5\text{E-}05$	168	$287.6 \pm 1.296$	$2.18 \pm 0.006$	95	0.999876
MCM-41, 2.0 nm	$\text{N}_2$ 77K	4.97E+05	$11.468 \pm 0.133$	$1.06\text{E-}01 \pm 3.5\text{E-}03$	$3.37\text{E-}02 \pm 1.8\text{E-}03$	13	$16.3 \pm 0.075$	$12.12 \pm 0.015$	80	0.999979
MCM-41, 4.5 nm	Ar 77K	8.08E+05	$2.053 \pm 0.002$	$2.00\text{E-}01 \pm 4.4\text{E-}03$	$3.67\text{E-}03 \pm 1.1\text{E-}04$	115	$226.4 \pm 1.035$	$3.46 \pm 0.012$	73	0.999907
macroporous silica	$\text{N}_2$ 77K	3.10E+05	$0.967 \pm 0.003$	$1.84\text{E-}01 \pm 7.2\text{E-}03$	$5.50\text{E-}02 \pm 5.1\text{E-}03$			$0.646 \pm 0.044$	102	0.999741
macroporous silica	Ar 87K	1.29E+04	$0.993 \pm 0.001$	$2.44\text{E-}01 \pm 3.3\text{E-}03$	$8.60\text{E-}03 \pm 6.0\text{E-}04$			$0.193 \pm 0.012$	119	0.999919

these values the fraction of molecules adsorbed with  $K_1$  has attained its final value. However, the total adsorption is given by the contribution of  $K_2$  to  $K_n$  in addition. Therefore  $Q_1$  cannot be assigned to a monolayer. The monolayer detection by the established but simplifying BET method yields  $240 \text{ cm}^3 \text{ g}^{-1}$  for  $\text{N}_2$  and  $237 \text{ cm}^3 \text{ g}^{-1}$  for Ar (cf. SI Fig. S8). When scientific doubts on the physical nature of the BET surface are set aside, a comparison of  $Q_1$  both derived from BET and the present model is possible. The deviation factor is 109 for  $\text{N}_2$  and 68 for Ar. With respect to the maximal cluster size of the primary sorption of  $\alpha = 168$  or 115 resp. the deviation factors are smaller than  $\alpha$  and eqn. (36) is fulfilled. The present model does not yet allow true surface area calculations. A theoretical approved method for the prediction of cluster geometries is required.

The parameters  $a$  and  $b$  listed in Table 1 are related to the cluster formation during the primary adsorption. For the adsorption of argon a dispersion potential with a distance-related exponent 6 is expected and due to eqns. (28) and (29) the exponent  $a$  is then  $6/3 = 2$  while the experimental value is about 0.2. That deviation underlines the principle difference of a flexible cluster compared to molecules. One may object that the parameter  $a$  is only possibly related to the presence of clusters but rather an empirical value with no meaning. Indeed it was a consensus in the literature that nitrogen and argon are adsorbed on siliceous MCM-41 in the primary state via layers [45, 46] although clusters of  $\text{N}_2$  and Ar can principally exist [47,48]. Only the high polar water is consistently assumed to be adsorbed via clusters in the early adsorption state [45,49]. However, recently the early cluster formation has been postulated as a result of Monte-Carlo simulations also for argon depending on the ratio of surface attraction and intermolecular forces [37,50,51]. Here, this ratio is defined by the quotient of  $a/b$ . It is 55 for argon, 25 for nitrogen with respect to its quadrupole moment and 3 for nitrogen in case of small pores. The energetic favor of clusters in the early sorption state should be greater the smaller that ratio is.  $\alpha$  and  $\beta$  represent the size of the clusters before and after the final capillary condensation step. They can directly be estimated from the isotherm figure. A spherical cluster with the size  $\beta = 288$  is calculated to have a diameter of 3.16 nm for liquid nitrogen ( $0.808 \text{ g cm}^{-3}$ ) which is 70% of the pore diameter. The MCM-41 with 2 nm pores is filled by one cluster to 60%. The reciprocal value of the final cluster formation constant  $K$  defines the position of the inflection point along the  $x$  axis.  $RT \ln K$  is a relative evaporation energy [3] and must directly depend on the pore size. According to Table 1, the constant  $K$  for the  $\text{N}_2$  sorption on 2 nm pores is significantly greater than that for 4.5 nm pores. More experiments related to that topic will be discussed in an upcoming publication.

### 3.5. Application to experimental type II isotherms

We will now proceed with the application of the new concept to type II isotherms. Often the modeling of type II isotherms is limited in its range. The BET isotherm [24] is practically, in case of surface area evaluation, restricted to the pressure segment between 0.05 and 0.3 [52]. More successful are the BET modification by Anderson [53], and the Frenkel-Halsey-Hill [1] equation. But in some cases, for example in the adsorption on macroporous silica, their application fails [54,55],

and even the employment of eqn. (1) of the preceding cluster model [3] generally proposed for type II by Ward [56] yields deviating results. The error of the last three isotherms is demonstrated here for the adsorption of nitrogen on macroporous silica [57] (SI, Figure S6). These tests are complemented by the Aranovich equation [66], alternatively derived from a lattice model. The fit is extremely bad, but substituting  $x$  with  $q$  yields quite better results.

When the General Cluster Sorption Isotherm (eqn. (18)) is applied to type II isotherms, the value of  $K$  defining the relative free energy of evaporation  $RT \ln K$  [3] is of interest. The position of  $1/K$  at the relative pressure axis of the isotherm is at  $x < 1$  for capillary condensation (type IV) but around  $x = 1$  in the unlimited condensation of type II open systems. However, analyzing sorption isotherms in the region of  $x$  between 0.98 and 1.0 is impaired by a principal strong increase of the experimental error [58]. The occurrence of a metastable equilibrium [59] during the condensation and additional condensation within the interstitial space of the particle bed are further problems. Hence, the interpretation of that isotherm region has to strongly rely on a theoretical basis. Both kinetic Monte-Carlo Simulation [59,60] and the theory of disjoining pressure [38,39] may help to understand that transition. Ward et al. [56,61] assumed that the isotherm passes through a point of inflection near  $x = 1$  and attains a hypothetical saturation value at  $x > 1$ . But this strategy is skipped and, in accordance with the BET theory [24], it is assumed here the absence of an inflection point. Instead, the isotherm is interpreted to go to infinite, not exactly at  $x = 1$ , but at  $q = 1$  according to Anderson's [53] BET modification. When using the present model given by the equations (18/19) we have to consider the principle existence of an inflection point somewhat below  $q = 1$ . The steepness of the curve at this point, however, is shifted upwards with increasing values of  $\beta$ . Since the experimental steepness cannot be measured exactly in this region, we assume that  $\beta$  tends to reach infinite. Hence infinite large clusters are formed during the condensation on the open adsorbent surface because of the absence of geometrical restrictions.

Let us look to eqn. (18). With  $\beta \rightarrow \infty$  the two  $\beta$  containing terms in the numerator cancel and the  $\beta$ -term in the denominator disappears for  $q < 1$ . Hence the isotherm equation is

$$\theta = \frac{(1-q)^2 \sum_{n=1}^{\alpha} n C_n q^n + q C_{\alpha} ((\alpha+1) q^{\alpha} - \alpha q^{\alpha+1})}{(1-q)^2 \left( 1 + \sum_{n=1}^{\alpha} C_n q^n \right) + (1-q) C_{\alpha} q^{\alpha+1}} \quad (39)$$

and only the series expansion up to the final natural number of  $n = \alpha$  remains. Compared to eqn. (18) describing type IV isotherm, the function above shows a completely different behavior at high values of  $q$ . Here finite values of  $\theta$  are restricted to  $0 \leq q < 1$  while at  $q \geq 1$  the value of the function is infinity. Regarding that definition of the singular state at  $q \geq 1$ , the transition of  $\beta \rightarrow \infty$  has also an impact on the steepness: while eqn. (18) has an inflection point at  $q \rightarrow 1$ , it is degenerated to a vertical asymptote at  $q \rightarrow 1$  (cf. SI).

Indeed, equation (39) seems to be only an artificial mathematical possibility: According to the present concept the cluster formation constants  $K_n$  decrease until the final value of  $K$  is reached. Lower values

are impossible. This must be the case at  $q = 1$ . Only for  $q > 1$  the cluster formation constant  $K$  is constant. However, it is a physical reality that the experimental type II isotherms span values up to only  $q = 1$ . The region  $q > 1$ , occurring in type IV, does not exist here. It is therefore impossible to attribute natural numbers of  $\alpha$  to infinite  $\beta$ . Simpler expressed, not only  $\beta$  but also  $\alpha$  have to approximate infinite which means mathematically that the  $\alpha$  terms of eqn. (39) cancel for  $q < 1$ , too. Hence the final equation for type II is

$$\theta = \frac{\sum_{n=1}^{\infty} n C_n q^n}{1 + \sum_{n=1}^{\infty} C_n q^n} \quad (40)$$

for  $q < 1$  where  $C_n$  is defined by the parameters  $a$  and  $b$  (eqn. (6) and (35)). That isotherm equation is identical with the general equation (7) of the cluster multi-equilibrium in section 3.1. apart from the upper limit of the series of expansion. To mark that this isotherm is more general than equation (7) it is denoted with  $\theta$  instead of  $\theta_\beta$ . For  $q \geq 1$   $\theta$  is found to be infinite (cf. SI) as previously mentioned for eqn. (39). The slope in the initial state is  $C_1$  as derived for  $\theta_\beta$  (cf. eqn. (20) and SI) so that Henry's condition is fulfilled. Another important limit is given by the surface tension  $\pi$  originating from Gibbs' law first introduced in eqns. (8) and (9).  $\pi$  can be calculated in the same manner for isotherms with  $\beta \rightarrow \infty$ .

$$\pi = RT \ln \left( 1 + \sum_{n=1}^{\infty} C_n q^n \right) \quad (41)$$

The surface tension has finite values only for  $q < 1$ . For  $q \geq 1$  the surface tension is infinite. Cassel [62,63] was the first pointing out the importance of that limit in case of the BET isotherm. When that isotherm approximates infinite at  $x \rightarrow 1$ , also the surface tension goes to infinite, although the surface tension has to be necessarily finite at  $x = 1$ . This is a serious fault of the BET equation, recalled later again by Hill [64] and Aranovich [65,66]. However, the present cluster based type II isotherm achieves that limit not at  $x = 1$  but at  $q = 1$ . Hence the condition  $K < 1$  has to be fulfilled, also according to Anderson's paper [53].

Fig. 4 shows the application of that new isotherm to the experimental data concerning the adsorption of nitrogen on macroporous silica [67].

While known isotherms fail (SI, Figure S6), an excellent fit is obtained here over a range of  $x = 10^{-6}$  to 0.99. The course of the  $K_n$  values given by eqn. (35) is shown by the grey curve of Fig. 2 starting with  $K_n$  values at  $K_1$  down to  $K$ .

Another example, presented here, concerns the adsorption of argon (87 K) on the same silica [68]. The isotherm fit is shown in the SI (Figure S7) and the resulting parameters are presented in Table 1.

The values of  $Q_1$ , representing the condition  $\theta = 1$ , are for  $N_2$ :  $Q_1 = 0.65$ , and for Ar:  $0.19 \text{ cm}^3 \text{ g}^{-1}$ . As already discussed earlier, these values cannot be attributed to a defined surface layer fraction. Only when one molecule is attached to the surface with  $K_1$  and the further clustering, proceeding with  $K_2$ ,  $K_2$  up to  $K_n$ , is positioned vertical to the surface, the value of  $Q_1$  would define the surface area. For comparison, the BET method in the pressure range  $0.05 < x < 0.2$  yields for  $N_2$ :  $Q_1 = 5.92$ , and for Ar:  $Q_1 = 5.23 \text{ cm}^3 \text{ g}^{-1}$  (SI, Fig. S9). The deviation factors are 8 and 27 and greater than unity according to eqn. (36).

The parameter  $a$  and  $b$  define the dependence of  $K_n$  on  $n$  and are in the same magnitude as those found for the siliceous mesoporous material. They make the essential difference towards the established theories of BET [24] and BET-derived [52] equations. The values of  $K$  are somewhat below unity so that Gibbs' integral is finite at  $x = 1$ .

### 3.6. Other types of isotherms

Up to now the application of the General Cluster Sorption Isotherm to type IV and type II isotherms has been discussed. Since type V isotherms can be regarded as a special case of type IV ( $K_1 < K$ ) [3], the new isotherm must be valid for type V, too. The main difference between these isotherms is the sign of the curvature in the beginning of the isotherm. It is defined by the second derivative at  $q = 0$ . As derived in the SI, this value depends only on  $C_1$  and  $C_2$ . A linear increase where the isotherm can be assigned as well to type VI and type V is defined by

$$C_1 = 2 C_2 \quad (42)$$

For type VI the condition

$$C_1 > 2 C_2 \quad (43)$$

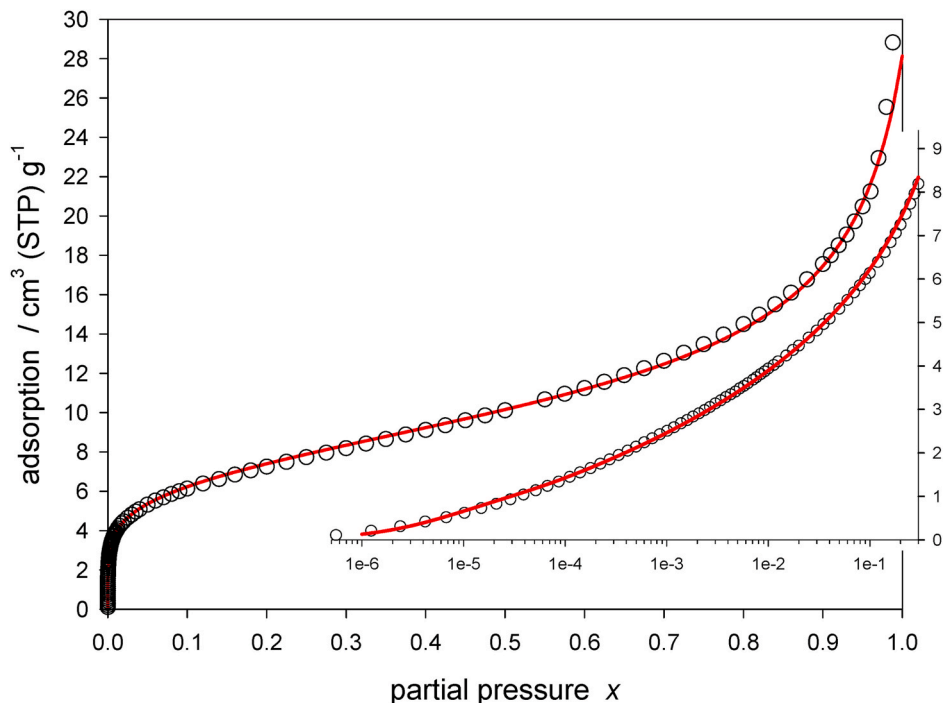


Fig. 4. Application of the General Cluster Sorption Isotherm (eqns. ((5), (35), (38) and (40)) to the adsorption of nitrogen (77 K) on macroporous silica [67].



and for type V

$$C_1 < 2 C_2 \quad (44)$$

has to be fulfilled. The higher members of  $C_n$  ( $n > 2$ ) have no influence. Analogous considerations hold for type III being a special case of type II. These types can be discriminated again by the ratio of  $C_1$  and  $C_2$  in the same manner as done by eqn. (42), (43) and (44).

Important special cases result when the decrease of  $K_n$  is extremely strong so that the members of  $K_n$  ( $n > 1$ ) contributing to the primary sorption state can be neglected. Eqn. (18) reduces then to eqn. (1) which has been introduced into the literature as  $\zeta$ -isotherm [20]. Beside this downgrading, that isotherm is also directly accessible starting with the general Klotz-equation (4), where instead of the sequence  $K_1, K_2, K_3, \dots, K_n$  only  $K_1$  is used to define the primary sorption step [3]. The  $\zeta$ -isotherm simplifies to Anderson's BET modification [52] for  $\beta \rightarrow \infty$ , to the  $n$ -layer BET equation [24] when  $K = 1$ , or to the common BET [24] when  $\beta \rightarrow \infty$  holds in addition. BET is reduced to Langmuir [69] for  $K = 0$ , and the highest degree of reduction is obtained when Henry's law (eqn. (20)) is reached. Mathematical transformations to these established classical isotherms can be followed up in the SI.

Within the group of important type II isotherms Aranovich's equation [66] requires special attention. That equation is similar to BET [24].

$$\theta(q) = \frac{C_1 x}{(1-x) \{1 + (C_1 - 1)x\}^m} \quad (45)$$

While the exponent  $m$  is 1 in case of BET, it ranges in between  $0 < m < 1$  in the Aranovich model. The main mismatch, however, is not the value of this exponent but the quite different theoretical background [65]. Within the BET multilayer concept each layer increases by the next without allowing vacancies in between. These vacancies are explicitly allowed in the lattice based concept of Aranovich. The present cluster concept comprises a freely chosen liquid-like ensemble of molecules of any shape where the average density defines the probability of holes. As outlined earlier within the introduction of equation (25) and (26), no freedom exists for "extra vacancies" inside a cluster. The average distance between the molecules is constant throughout the total isotherm. The only allowed variable vacancy is the separating space between clusters. Therefore, the present model is only partially congruent with Aranovich's recursion on the Kondo-Ono lattice [74]. Nevertheless, it would be interesting to look for a theory which can combine these two worlds.

Not yet mentioned were stepwise type VI isotherms. If not occurring as a result of an additive superposition of several distinct sites of adsorption, the interpretation of these isotherms, when occurring on homogeneous surfaces [70,71], can be explained by the assumption of several phase transitions [72,73]. This requires an extension of eqn. (18): In case of a 2-step VI isotherm after the first phase transition at  $\alpha$  with  $K = K_I$  a second occurs with  $K = K_{II}$  at  $\beta$  up to the maximal clustering at  $\gamma$ .

#### 4. Conclusion

The General Cluster Sorption Isotherm is a coherent mathematical treatment of thermodynamic equilibria constituting the formation of flexible clusters. Its main feature is that the sorbate-sorbate interaction is not restricted on an orientation vertical to the adsorbent surface as commonly underlain to multilayer isotherms. It is not necessary that the clusters are separated from each other: they may exist as separated surface attached clusters, but they may also merge and form mono- and multilayers or a pore filling liquid in case of capillary condensation. In order to predict the preference of isolated cluster-islands against continuous multilayers including its impact on hysteresis, further studies are required to calculate local surface tension, based on simulation and additional physical data.

The General Cluster Sorption Isotherm has been developed as an

extension of an earlier approach [3] describing the influence of capillary condensation on adsorption isotherms. While the application of the latter concept is restricted to adsorbates highly interacting with itself but with low affinity to the surface, the present model is successfully tested for those type IV isotherms with lower sorbate-sorbate interaction where the earlier concept fails. Instead of describing the adsorbent-surface interaction with only one parameter, a sequence of parameters  $C_1, C_2, C_3 \dots C_n$  is introduced. These parameters are interpreted to be the result of an energy relationship. Depending on the degree of cluster size  $n$  the surface-cluster interaction including the cluster formation energy is proportional to the product of  $n+1$  power functions

$$\varepsilon_n \propto n^{-a} \times (n^{-b})^n$$

Although theoretically not fully understood, this relationship can serve as an alternative to molecular distance-based LJ potentials used in classical DFT concepts. Here, the flexible cluster approach results in energy contributions which are multiplied with each other, while the focus on only single molecules in DFT engenders additive contributions.

The resulting full isotherm is not expressed by a single mathematical equation. Numerical analysis of experimental data requires  $\theta = f(K, \alpha, \beta, C_1, C_2, C_3, \dots C_n)$  combined with  $C_n = f(K_1, a, b)$ . These equations are found to describe the adsorption of nitrogen and argon on two types of ordered mesoporous silica in the partial pressure range from  $10^{-6}$  up to more than 0.7. The fit is better than that obtained by NLDFT and comparable with the accuracy of QSDFT isotherms. An application to further type IV adsorption data including the evaluation and interpretation of the specific model parameters is therefore of strong interest.

The General Cluster Sorption Isotherm can be reduced to a form without capillary condensation. The resulting equation, with a cluster size approximating infinity at a partial pressure near unity, describes type II isotherms. In contrast to BET and other multilayer isotherms, the present concept is found to be applicable to a wide partial pressure range from  $10^{-6}$  to 1 in case of nitrogen and argon on macroporous silica.

The isotherm for type II contains a characteristic sequence of  $C_n$  values up to  $n \rightarrow \infty$ . When  $C_n$  is reduced to only a single value  $C = C_1$  and the constant  $K$  is unity, the General Cluster Sorption Isotherm merges with the well known BET equation [24]. Nevertheless BET is broadly used in science for surface area determination, mostly on the basis of only few experimental points, far beyond to represent the full isotherm. Such surface areas can characterize different adsorbents relative to each other, but the true surface area is another matter. However, a progress in the solution of that problem cannot be deduced from the present sorption isotherm because the geometry and therefore the specific surface area of the flexible cluster is yet unknown.

The present model can only be validated by adsorption on a homogeneous surface. This prerequisite is fulfilled for mesoporous and macroporous silica but not for irregular microporous materials such as microporous carbon. Adsorption on such materials has to be regarded as an additive superposition of isotherms for homogeneous patches. Respective calculations of the adsorbent's characteristic energy distributions have been reported on the basis of homogeneous Langmuir isotherms [6]. The transfer of that approach to precisely measured cluster isotherms is surely possible but the number of fit parameters combined with the calculation of power series inside a large span between very small and very large numbers is expected to be a challenge for numerical processing.

Integration of several isotherms is also required for pore size calculations. The parameter  $K$ , marking the position of capillary condensation, has to depend on the pore diameter. The General Cluster Sorption Isotherm is therefore expected to be a principle basis for pore size determinations.

Since type IV isotherms can principally be reduced (or extended) to all other types of isotherms, the present concept seems to be universal. This statement also holds when the energy distribution function is criticized to be only empirical.

## CRediT authorship contribution statement

**Christoph Buttersack:** Conceptualization, Data curation, Theory, Software, Programming, Validation, Writing - original draft.

## Declaration of competing interest

The author declares that he has no known competing financial interests or personal relationships that could have appeared to influence the work reported in this paper.

## Acknowledgement

I thank Prof. Dr. Michal Kruk of the City University of New York for providing me with original data files concerning the adsorption of nitrogen and argon on siliceous MCM-41 samples in the relative pressure range of  $10^{-6}$  to 0.99.

I thank Prof. Dr. Siegfried Carl of the Martin-Luther University of Halle, Germany, Institute of Mathematics, for checking the mathematical transformations and help in function analysis.

## Appendix A. Supplementary data

Supplementary data to this article can be found online at <https://doi.org/10.1016/j.micromeso.2021.110909>.

## References

- [1] D.D. Do, Adsorption Analysis: Equilibria and Kinetics, Imperial College Press, 1998.
- [2] L. Sarkisov, A. Centineo, S. Brandani, Molecular simulation and experiments of water sorption in surface activated carbon, *Carbon* 118 (2017) 127–138.
- [3] C. Buttersack, Modeling of type IV and V isotherms, *Phys. Chem. Chem. Phys.* 21 (2019) 5614–5626.
- [4] K.S. W Sing, D.H. Everett, R.A.W. Haul, L. Moscou, R.A. Pierotti, J. Rouquerol, T. Siemieniowska, Reporting physisorption data for gas/solid systems, *Pure Appl. Chem.* 57 (1985) 603–619.
- [5] W. Rudzinski, D.H. Everett, Adsorption of Gases on Heterogeneous Surfaces, Academic Press, San Diego, 1992.
- [6] K.C. Ng, M. Burhan, M.W. Shahzad, A.B. Ismail, A universal isotherm model to capture adsorption uptake and energy distribution of porous heterogeneous surface, *Sci. Rep.* 7 (2017) 10634.
- [7] M. Burhan, M.W. Shahzad, K.C. Ng, A universal theoretical framework in material characterization for tailored porous surface design, *Sci. Rep.* 9 (2019) 8773.
- [8] J. Landers, G.Y. Gor, A.V. Neimark, Density functional theory methods for characterization of porous materials, *Colloids Surf., A* 437 (2013) 3–32.
- [9] P. Tarazona, U.M. Marconi, R. Evans, Phase equilibria of fluid interfaces and confined fluids. Non-local versus local density functionals, *Mol. Phys.* 60 (1987) 573–595.
- [10] P.I. Ravikovitch, A.V. Neimark, Density functional theory model of adsorption on amorphous and microporous silica materials, *Langmuir* 22 (2006) 11171–11179.
- [11] A.V. Neimark, Y. Lin, P.I. Ravikovitch, M. Thommes, Quenched solid density functional theory and pore size analysis of micro-mesoporous carbons, *Carbon* 47 (2009) 1617–1628.
- [12] G.Y. Gor, M. Thommes, K.A. Cychoz, A.V. Neimark. Quenched solid density functional theory method for characterization of mesoporous carbons by nitrogen adsorption. *Carbon* 50 (201102) 1583–1590.
- [13] R.T. Cimino, P. Kowalczyk, P.I. Ravikovitch, A.V. Neimark, Determination of isosteric heat of adsorption by quenched solid density functional theory, *Langmuir* 33 (2017) 1769–1779.
- [14] L. Liu, S. Tan, T. Horikawa, D.D. Do, D. Nicholson, J. Liu. Water adsorption on carbon, A review. *Adv. Coll. Interf. Sci.* 250 (2017) 64–78.
- [15] M.C. Verbracke, S. Brandani, A priori predictions of type I and type V isotherms by the rigid adsorbent lattice fluid, *Adsorption* (2019), <https://doi.org/10.1007/s10450-019-00174-7>.
- [16] I.M. Klotz, F.M. Walker, R.B. Pivan, The binding of organic ions by proteins, *J. Am. Chem. Soc.* 68 (1946) 1486–1490.
- [17] I.M. Klotz, Protein interactions with small molecules, *Acc. Chem. Res.* 7 (1974) 162–168.
- [18] L. Michaelis, M.L. Menten, Die Kinetik der Invertinwirkung, *Biochem. Z.* 49 (1913) 333–369.
- [19] K.A. Johnson, R.S. Goody, The original Michaelis constant: translation of the 1913 Michaelis-Menten paper, *Biochemist* 50 (2011) 8264–8269.
- [20] C.A. Ward, J. Wu, Effect of adsorption on the surface tensions of solid-fluid interfaces, *J. Phys. Chem. B* 111 (2007) 3685–3694.
- [21] W.H. Press, B.P. Flannery, S.A. Teukolsky, W.T. Vetterling, Numerical Recipes, Cambridge University Press, 1986.
- [22] R core team, A Language and Environment for Statistical Computing, R foundation for statistical computing, Vienna, Austria, 2017. URL, <https://www.R-project.org/>.
- [23] T.V. Elzhov, K.M. Mullen, A.N. Spiess, B.M. Bolker, R Interface to the Levenberg-Marquardt Nonlinear Least-Squares Algorithm Found in MINPACK, 2016. <https://cran.r-project.org/web/packages/minpack.lm/minpack.lm.pdf>.
- [24] S. Brunauer, P.H. Emmett, E. Teller, Adsorption of gases in multimolecular layers, *J. Am. Chem. Soc.* 60 (1938) 309–319.
- [25] J.R. Pliego, J.M. Riveros, Hybrid discrete-continuum solvation methods, *WIREs Comp. Mol. Sci.* 10 (2020) e1440.
- [26] A.D. Poulikas (Ed.), The Transforms and Applications Handbook, CRC-Press, 1996, p. 1022. , 5th equation.
- [27] I.N. Bronshtein, K.A. Semendiyayev, G. Musiol, H. Mühlig (Eds.), Handbook of Mathematics, 6th ed., Springer, 2015, p. 19.
- [28] J.A. Israelachvili, Intermolecular and Surface Forces, Academic Press, 2013.
- [29] R.M. Richard, K.U. Lao, J.M. Herbert, Aiming for benchmark accuracy with the many-body expansion, *Acc. Chem. Res.* 47 (2014) 2828–2836.
- [30] Ref 28, Chapter 10, Unifying Concepts in Intermolecular and Interparticle Forces, p.191.
- [31] E. Zappa, M. Holmes-Cerfon, Calculating the symmetry number of flexible sphere clusters, *J. Nonlinear Sci.* 29 (2019) 2021–2053.
- [32] J.D. Evans, G. Fraux, R. Gaillac, D. Kohen, F. Trousset, J.M. Vanson, F.X. Coudert, Computational methods for nanoporous materials, *Chem. Mater.* 29 (2017) 199–212.
- [33] D.D. Do, H.D. Do, D. Nicholson, A computer appraisal of BET theory, BET surface area and the calculation of surface excess for gas adsorption on a graphite surface, *Chem. Eng. Sci.* 65 (2010) 3331–3340.
- [34] M.F. de Lange, L.C. Lin, J. Gascon, T.J.H. Vlugt, F. Kapteijn, Assessing the surface area of porous solids: limitations, probe molecules, and methods, *Langmuir* 32 (2016) 12664–12675.
- [35] A. Datar, Y.G. Chung, L.C. Lin, Beyond the BET analysis: the surface area prediction of nanoporous materials using a machine learning method, *J. Phys. Chem. Lett.* 11 (2020) 5412–5417.
- [36] M. Thommes, K. Kaneko, A.V. Neimark, J.P. Olivier, F. Rodriguez-Reinoso, J. Rouquerol, K.S.W. Sing, Physisorption of gases, with special reference to the evaluation of surface area and pore size distribution (IUPAC technical report), *Pure Appl. Chem.* 87 (2015) 1051–1069.
- [37] L. Prasetyo, Q.K. Loi, S.J. Tan, D.D. Do, D. Nicholson, Effects of temperature on the transition from clustering to layering for argon adsorption on substrates of different strengths - parametric map of wetting, pre-wetting and non-wetting, *Microporous Mesoporous Mater.* 304 (2020) 109239.
- [38] D. Wasan, A. Nicolov, K. Kondiparty, The wetting and spreading of nanofluids on solids: the role of structural disjoining pressure, *Curr. Opin. Colloid Interface Sci.* 15 (2011) 344–349.
- [39] J. Adolphs, Thermodynamics and modeling of sorption isotherms, *Chem. Ing. Tech.* 88 (2016) 274–281.
- [40] M. Kruk, M. Jaroniec, Y. Sakamoto, O. Terasaki, R. Ryoo, C.H. Ko, Determination of pore size and pore wall structure of MCM-41 by using nitrogen adsorption, transmission electron microscopy, and X-ray diffraction, *J. Phys. Chem. B* 104 (2000) 292–301.
- [41] C.Y. Chen, H.X. Li, M.E. Davis, Studies on mesoporous materials. Synthesis and characterization of MCM-41, *Microporous Mater.* 2 (1993) 17–26.
- [42] M. Kruk, M. Jaroniec, A. Sayari, Application of large pore MCM-41 molecular sieves to improve pore size analysis using nitrogen adsorption measurements, *Langmuir* 13 (1997) 6267–6273.
- [43] M. Kruk, M. Jaroniec, Determination of mesopore size distributions from argon adsorption data at 77 K, *J. Phys. Chem. B* 106 (2002) 4732–4739.
- [44] K. Schappert, R. Pelster, Elastic properties and freezing of argon confined in mesoporous glass, *Phys. Rev. B* 78 (2008) 174108.
- [45] F.R. Hung, S. Bhattacharya, B. Coasne, M. Thommes, K. Gubbins, Argon and krypton adsorption on templated mesoporous silicas: molecular simulation and experiment, *Adsorption* 13 (2017) 425–437.
- [46] S.C. Chang, S.Y. Chien, C.L. Chen, C.K. Chen, Analyzing adsorption characteristics of CO<sub>2</sub>, N<sub>2</sub>, and H<sub>2</sub>O in MCM-41 silica by molecular simulation, *Appl. Surf. Sci.* 331 (2015) 225–233.
- [47] T.N. Gribanova, A.A. Milov, A.G. Starikov, O.A. Gapurenko, V.A. Gurashvili, R. M. Minyaev, V.I. Minkin, Cooperative effects in polymolecular nitrogen clusters, *Russ. Chem. Bull.* 57 (2008) 2037.
- [48] H.Y. Tang, I.A. Ford, Free energies of molecular clusters determined by guided mechanically disassembly, *Phys. Rev.* 91 (2015), 023308.
- [49] T. Ohba, H. Kanoh, K. Kaneko, Cluster-growth-induced water adsorption in hydrophobic carbon nanopores, *J. Phys. Chem. B* 108 (2004) 14964–14969.
- [50] J.H. Pu, J. Sun, Q. Sheng, W. Wang, H.S. Wang, Dependences of formation and transition of the surface condensation mode on wettability and temperature, *Langmuir* 36 (2020) 456–464.
- [51] X. Wei, C.M. Wu, Y.R. Li, Molecular insight into the formation of adsorption clusters based on the zeta isotherm, *Phys. Chem. Chem. Phys.* 22 (2020) 10123–10131.
- [52] R. Bardestani, G.S. Patience, S. Kalaguine, Experimental methods in chemical engineering: specific surface area and pore size distribution measurements - BET, BJH, and DFT, *Can. J. Chem. Eng.* 97 (2019) 2781–2791.
- [53] R.B. Anderson, Modification of the Brunauer, Emmett and Teller equation, *J. Am. Chem. Soc.* 68 (1946) 686–691.
- [54] G.Y. Gor, O. Paris, J. Prass, P. Russo, M. Manuela, R. Carrott, A.V. Neimark, Adsorption of n-pentane on mesoporous silica and adsorbent deformation, *Langmuir* 29 (2013) 8601–8608.

- [55] P.J.M. Carrott, R.A. Roberts, K.W.S. Sing, Adsorption of neopentane by nonporous carbons and silica, *Langmuir* 4 (1988) 740–743.
- [56] N. Narayanaswamy, C.A. Ward, Specific surface area, wetting, and surface tension of materials from N<sub>2</sub> vapor adsorption isotherms, *J. Phys. Chem. C* 123 (2019) 18336–18346.
- [57] M. Jaroniec, M. Kruk, J.P. Olivier, Standard adsorption data for characterization of nanoporous silicas, *Langmuir* 15 (1999) 5410–5413.
- [58] J.B. Condon, Chapt. 2, Measuring physisorption isotherms. *Surface Area and Porosity Determinations by Physisorption*, Elsevier, 2020, pp. 74–77. , Figure 2.4.
- [59] R. Godawat, S.N. Jamadagni, J.R. Errington, S. Garde, Structure, stability, and rupture of free and supported liquid films and assemblies in molecular simulations, *Ind. Eng. Chem. Res.* 47 (2008) 3582–3590.
- [60] S. Tan, Q.K. Loi, D.D. Do, D. Nicholson, On the canonical isotherms for bulk fluid, surface adsorption and adsorption in pores, *J. Colloid Interface Sci.* 548 (2019) 25–36.
- [61] S. Yaghoubian, S.H. Zandavi, C.A. Ward, From adsorption to condensation: the role of adsorbed molecular clusters, *Phys. Chem. Chem. Phys.* 18 (2016) 2181–21481.
- [62] H.M. Cassel, Condensation and super-saturation of adsorbed phases, *J. Chem. Phys.* 12 (1944) 115–116.
- [63] H.M. Cassel, Cluster formation and phase transitions in the adsorbed state, *J. Phys. Chem.* 48 (1944) 195–202.
- [64] T.L. Hill, *An Introduction to Statistical Thermodynamics*, Addison-Wesley, 1960, p. 135.
- [65] G.L. Aranovich, The theory of polymolecular adsorption, *Langmuir* 8 (1992) 736–739.
- [66] G.L. Aranovich, A new approach to analysis of multilayer adsorption, *J. Colloid Interface Sci.* 173 (1995) 515–520.
- [67] M. Jaroniec, M. Kruk, J.P. Olivier, Standard adsorption data for characterization of nanoporous silicas, *Langmuir* 15 (1999) 5410–5413.
- [68] M. Kruk, M. Jaroniec, Accurate method for calculating mesopore size distributions from argon adsorption data at 87 K developed using model MCM-41 material, *Chem. Mater.* 12 (2000) 222–230.
- [69] I. Langmuir, The adsorption of gases on plane surfaces of glass, mica, and platinum, *J. Am. Chem. Soc.* 40 (1918) 1361–1403.
- [70] S.J. Gregg, S.J.K.S.W. Sing, *Adsorption, Surface Area and Porosity*, Academic Press, 1982, pp. 84–89.
- [71] D. Nicholson, R.G. Silvester, Investigation of step formation in multilayer adsorption isotherms using a lattice model, *J. Colloid Interface Sci.* 62 (1977) 447–453.
- [72] A. Boutin, R.J.M. Pellenq, D. Nicholson, Molecular simulation of stepped adsorption isotherm of methane in AlPO<sub>4</sub>-5, *Chem. Phys. Lett.* 219 (1994) 484–490.
- [73] M.B. Yahia, Y.B. Torkia, S. Knani, M.A. Hachicha, M. Khalfaouchi, A.B. Lamine, Models for type VI adsorption isotherms from a statistical mechanical formulation, *Adsorpt. Sci. Technol.* 31 (2013) 341–357.
- [74] S. Ono, S. Kondo, Molecular theory of surface tension in liquids, in: H.S. Green, S. Ono, S. Kondo, F.P. Buff (Eds.), *Encyclopedia of Physics*, 3, Springer, Göttingen, 1960, pp. 134–280.